11 May 2026

Leveling up upconverting nanoparticles with machine learning

Ripeng Luo[1,2], Jungmin Hamm[1], Emory M Chan[1]

1. The Molecular Foundry, Lawrence Berkeley National Laboratory

2. Department of Materials Science and Engineering, University of California

Abstract

Upconverting nanoparticles (UCNPs) transform low-energy light into higher-energy photons, enabling applications in subwavelength and subsurface imaging, nanoscale sensing, therapeutics, optogenetics, printing, and optical computing. However, the widespread adoption of UCNPs is hindered by their low brightness and limited spectral tunability. Predicting the ideal nanoparticle architectures to overcome these limitations is challenging, because UCNP photophysics are governed by highly nonlinear, complex energy transfer networks that span the excited states of lanthanide dopants. Due to the large number of possible combinations of dopants, concentrations, host matrices, heterostructures, and reaction conditions, optimizing the compositional and synthetic parameters of UCNPs using conventional trial-and-error approaches is intractable.This Account explores how researchers can overcome these challenges and enhance the properties of UCNPs using artificial intelligence (AI) and machine learning (ML). We first review how the early foundations of AI-guided discovery were established with automated experimental workflows and physical modeling. Using robotic synthesis platforms and differential rate equation models, researchers have successfully navigated high-dimensional compositional spaces to reveal optical phenomena such as energy-looping and photon avalanching in nanoparticles.Building on these data-driven approaches, ML was integrated into UCNP research initially for processing raw characterization data, such as automating the analysis of TEM images and time-resolved luminescence curves. AI approaches were extended to interpret signals in applications that utilize UCNPs, such as classifying the cytotoxicity of drugs based on upconversion luminescence microscopy data. Most significantly, ML is driving the design of new UCNP compositions and structures, including our recent development of closed-loop active learning of UCNP core-shell heterostructures. By coupling Bayesian optimization with kinetic Monte Carlo (kMC) simulations, we achieved 110-fold enhancement in UCNP emission over just 40 iterations. To bypass the

steep computational cost of simulating UCNP heterostructures with up to 9 shells, we leveraged differentiable deep learning surrogate models based on heterogeneous graph neural networks to perform inverse design. Notably, these hetero-GNNs were able to extrapolate far outside of the model's training data and predict UCNP heterostructure compositions with 6.5-fold more intense emission than the brightest UCNP in the training set.In the future, we predict that AI/ML approaches will become integral to UCNP research. UCNP experiments may soon be accelerated by autonomous self-driving laboratories in which robotic synthesis, in-line characterization, and ML agents operate in a closed feedback loop to intelligently investigate underexplored chemical spaces. Large language models (LLMs) could parse literature to develop overarching hypotheses and detailed recipes for these autonomous workflows, with generative models suggesting novel structures to test. Together with human creativity and critical analysis, these AI tools will accelerate the discovery of advanced upconverting nanomaterials, aiding fundamental understanding of their mechanisms, and inspiring a broader array of photonic applications.

Keywords

Upconversion, nanoparticles, machine learning, artificial intelligence

Leveling up upconverting nanoparticles with machine learning

Ripeng Luo, [‡1,2] Jungmin Hamm, [‡1] and Emory M. Chan[1*]

[1]*The Molecular Foundry, Lawrence Berkeley National Laboratory, Berkeley, California 94720, United States*

[2]*Department of Materials Science and Engineering, University of California, Berkeley, California 94720, United States*

[‡] *These authors contributed equally to this work.*

* To whom correspondence should be addressed. E-mail: emchan@lbl.gov

Keywords: Upconversion, nanoparticles, machine learning, artificial intelligence

Conspectus:

Upconverting nanoparticles (UCNPs) transform low-energy light into higher-energy photons, enabling applications in subwavelength and subsurface imaging, nanoscale sensing, therapeutics, optogenetics, printing, and optical computing. However, the widespread adoption of UCNPs is hindered by their low brightness and limited spectral tunability. Predicting the ideal nanoparticle architectures to overcome these limitations is challenging, because UCNP photophysics are governed by highly nonlinear, complex energy transfer networks that span the excited states of lanthanide dopants. Due to the large number of possible combinations of dopants, concentrations, host matrices, heterostructures, and reaction conditions, optimizing the compositional and synthetic parameters of UCNPs using conventional trial-and-error approaches is intractable.

This Account explores how researchers can overcome these challenges and enhance the properties of UCNPs using artificial intelligence (AI) and machine learning (ML). We first review how the early foundations of AI-guided discovery were established with automated experimental workflows and physical modeling. Using robotic synthesis platforms and differential rate equation models, researchers have successfully navigated high-dimensional compositional spaces to reveal optical phenomena such as energy-looping and photon avalanching in nanoparticles.

Building on these data-driven approaches, ML was integrated into UCNP research initially for processing raw characterization data, such as automating the analysis of TEM images and time-resolved luminescence curves. AI approaches were extended to interpret signals in applications that utilize UCNPs, such as classifying the cytotoxicity of drugs based on upconversion luminescence microscopy data. Most significantly, ML is driving the design of new UCNP compositions and structures, including our recent development of closed-loop active learning of UCNP core-shell heterostructures. By coupling Bayesian optimization with kinetic Monte Carlo (kMC) simulations, we achieved 110-fold enhancement in UCNP emission over just 40 iterations. To bypass the steep computational cost of simulating UCNP heterostructures with up to 9 shells, we leveraged differentiable deep learning surrogate models based on heterogeneous graph neural networks to perform inverse design. Notably, these hetero-GNNs were able to extrapolate far outside of the model's training data and predict UCNP heterostructure compositions with 6.5-fold more intense emission than the brightest UCNP in the training set.

In the future, we predict that AI/ML approaches will become integral to UCNP research. UCNP experiments may soon be accelerated by autonomous self-driving laboratories in which robotic synthesis, in-line characterization, and ML agents operate in a closed feedback loop to intelligently investigate underexplored chemical spaces. Large language models (LLMs) could parse literature to develop overarching hypotheses and detailed recipes for these autonomous workflows, with generative models suggesting novel structures to test. Together with human creativity and critical analysis, these AI tools will accelerate the discovery of advanced upconverting nanomaterials, aiding fundamental understanding of their mechanisms, and inspiring a broader array of photonic applications.

Key References

- Chan, E. M.; Han, G.; Goldberg, J. D.; Gargas, D. J.; Ostrowski, A. D.; Schuck, P. J.; Cohen, B. E.; Milliron, D. J. Combinatorial Discovery of Lanthanide-Doped Nanocrystals with Spectrally Pure Upconverted Emission. *Nano Lett.* **2012**, *12* (7), 3839-3845.
- Qi, X.; Lee, C.; Ursprung, B.; Skripka, A.; Schuck, P. J.; Chan, E. M.; Cohen, B. E. Short-Wave Infrared Upconverting Nanoparticles. *Journal of the American Chemical Society* **2024**, *146* (43), 29292-29296.
- Xia, X.; Sivonxay, E.; Helms, B. A.; Blau, S. M.; Chan, E. M. Accelerating the Design of Multishell Upconverting Nanoparticles through Bayesian Optimization. *Nano Lett.* **2023**, *23* (23), 11129-11136.
- Sivonxay, E.; Attia, L.; Spotte-Smith, E. W. C.; Sanchez-Lengeling, B.; Xia, X.; Barter, D.; Chan, E. M.; Blau, S. M. Gradient-based optimization of complex nanoparticle heterostructures enabled by deep learning on heterogeneous graphs. *Nature Computational Science* **2026**, *6* (1), 83-95.

1. Introduction

Upconverting nanoparticles[1-5] (UCNPs) combine the energy absorbed from two or more low-energy photons into the emission of a high-energy photon.[6, 7] This step-wise, multiphoton process is valuable for applications where near-infrared light is beneficial for minimizing scattering and photodamage, but where conversion to shorter wavelengths is needed for efficient detection[8] (e.g., for night vision[2, 9]) or to stimulate photochemistry (e.g., for optogenetics,[10, 11] therapeutics,[12-15] and lithography[16]). The exceptional photochemical stability of UCNPs is a critical feature that enables extended tracking of single particles,[17-20] nanoscale sensing,[21-24] and continuous-wave lasing,[25-27] while the high nonlinearity of UCNPs and photon avalanching nanoparticles[28-32] is leveraged for subwavelength imaging[30, 33, 34] and optical computing.[35, 36]

The widespread adoption of such applications is currently limited by several key challenges, most significantly the low brightness of UCNPs compared to conventional fluorophores.[37] The high laser power densities (10^1-10^6 W/cm^2) needed to compensate for the low quantum yields of UCNPs (ca. 1%) discourage their application in photosensitive environments.[38] UCNPs also face challenges with their long luminescence lifetimes, limited tunability of their excitation[2, 39] and emission wavelengths,[1] and large size relative to the processes they probe.[19, 20]

Thus, a major objective of UCNP research is to discover new compositions and structures that overcome these limitations.[37] UCNPs with ideal properties, however, are difficult to predict because their photophysics are driven by complex energy transfer (ET) networks among the excited states of the lanthanide dopants.[40] To tune UCNP properties, researchers historically have relied on trial-and-error approaches, modulating the combination and concentration of lanthanide dopants,[1] modifying host crystal matrices (typically $NaYF_4$),[41-43] partitioning dopants across heterostructures,[44-46] and coupling UCNPs to ligands,[8, 47] dyes,[10, 48, 49] and plasmonic structures.[26] Systematic screening of these compositions is complicated by the fact that UCNP properties are highly dependent on synthesis conditions.[50] The large number of variables in such many-component structures leads to millions of possible combinations to explore, turning the search for optimal candidates into a high-dimensional optimization problem that is experimentally intractable[7] even with high-throughput automated approaches developed in our group.[1, 51] Even simulations[4, 40, 52] are prohibitively expensive at large system sizes.[53]

With the current boom in artificial intelligence (AI), machine learning (ML) and data-driven approaches in principle could be used to improve UCNP properties and enhance fundamental understanding of upconversion phenomena. ML models are already being used to predict materials properties,[54, 55] design experiments for self-driving autonomous laboratories,[56-58] and generate new materials to explore. These methods have been extended to colloidal nanoparticle systems[50, 59] such as semiconductor quantum dots,[60-62] perovskites,[63, 64] metals,[65, 66] and their complex heterostructures.[67] However, ML has been used only sparingly to investigate UCNPs, leaving its potential untapped. It is an open question whether AI/ML approaches can lead to the discovery of genuinely new upconverting materials or understanding. In this Account, we review recent applications of AI to UCNPs (Figure 1) and discuss how ML can truly "level up" research into upconverting nanomaterials.

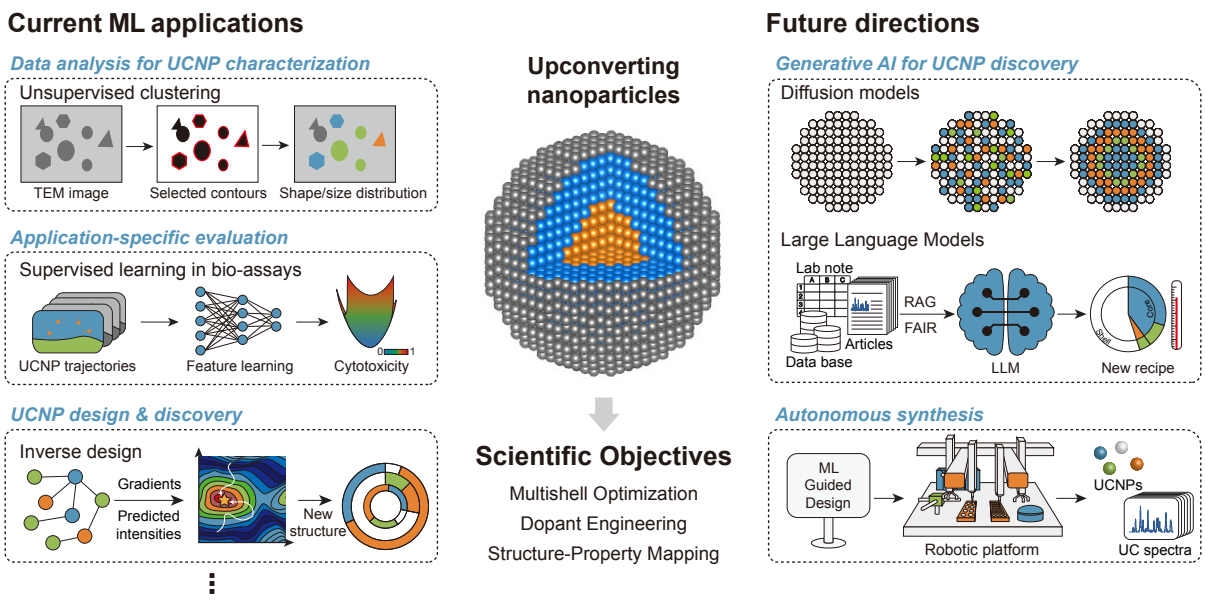

Figure 1. Overview of ML in UCNP research, including applications, objectives, and future directions.

2. Are UCNPs ready for ML?

Are UCNPs an appropriate platform for ML-guided optimization and discovery? AI approaches excel for complex problems that cannot be solved analytically, using simple deduction (e.g., varying a single dopant concentration), or using basic heuristics ("high dopant concentration quenches emission"). UCNP investigations fit this profile because, like common ML problems, UCNPs have many components (e.g. dopants, host matrices, and subdomains) that are coupled through highly nonlinear relationships,[7] such as the complex ET networks among lanthanide dopants.[40] Such high-dimensional problems cannot be solved by brute force experimentation due to its prohibitive cost and due to noisy, rough response surfaces.[4] Like the best ML problems, UCNP research often features well-defined objectives,[7] such as optimizing brightness, recommending synthesis steps, or interpreting biological assays. There is also ample room for ML algorithms to improve UCNPs because baseline efficiencies are low[38] and performance spans orders of magnitude.[1, 2, 68] ML also promises to discover and optimize UCNPs more efficiently than conventional workflows since the optimal solutions are often found in tiny regions in high-dimensional parameter space that are underexplored due to human bias.[69]

Is there enough high-quality UCNP data for ML? ML models typically require large quantities of training data. These data must be sufficiently reproducible and readily comparable across experiments, since variations in synthesis protocols, measurement conditions, and reporting formats can limit robust ML analysis. With their rapid optical readout and chemically interchangeable but electronically diverse lanthanide dopants, UCNPs are ideal platforms for generating large combinatorial libraries.[7] We and others have demonstrated robotic[51, 70, 71] and microfluidic[72] workflows that can produce expansive, ML-ready datasets through the high-throughput synthesis of UCNPs[1] and programmed growth of multi-shell, lanthanide-doped heterostructures.[46, 73] The ability to calculate approximate UCNP spectra facilitates the validation and pre-training of new ML algorithms using computational data prior to expensive experimental campaigns. We have successfully generated over 200,000 UCNP spectra[2] using differential rate equation calculations (DREs)[52] and simulated over 30,000 spectra of multi-shell UCNP heterostructures[4] using kinetic Monte Carlo (kMC).[3, 40, 74] Crucially, ML remains attractive because DRE models are limited in complexity, and kMC becomes computationally prohibitive for large UCNPs.

Previous data-driven approaches for UCNPs. Even before their integration with ML, high-throughput computational and experimental methods have accelerated the discovery of new UCNP structures, the development of computational methods, the elucidation of ET pathways, and the observation of novel optical phenomena. In 2010, we demonstrated automated UCNP synthesis using WANDA,[51] the first reported nanocrystal synthesis robot. Screening UCNPs doped with every combination of up to three lanthanide co-dopants yielded comprehensive datasets[1] used to develop a computational DRE package predicting the luminescence of NPs with any combination of lanthanide dopants.[52] We utilized these tools to predict UCNPs optimized for single particle imaging[20] and short-wave infrared excitation.[2] High-throughput computational screening for UCNPs excitable at 1064 nm identified energy looping Tm^{3+}-doped $NaYF_4$ nanoparticles,[68] which were subsequently refined with WANDA to discover photon avalanching nanoparticles (ANPs).[30] These ANPs exhibit optical nonlinearities exceeding 30, enabling the realization of new modes of super-resolution imaging,[30, 33, 34] photoswitching,[33, 35] and sensing.[21, 22, 75] These examples demonstrate that high-throughput, data-driven workflows have underpinned major advances in UCNPs and are primed for integration with ML.

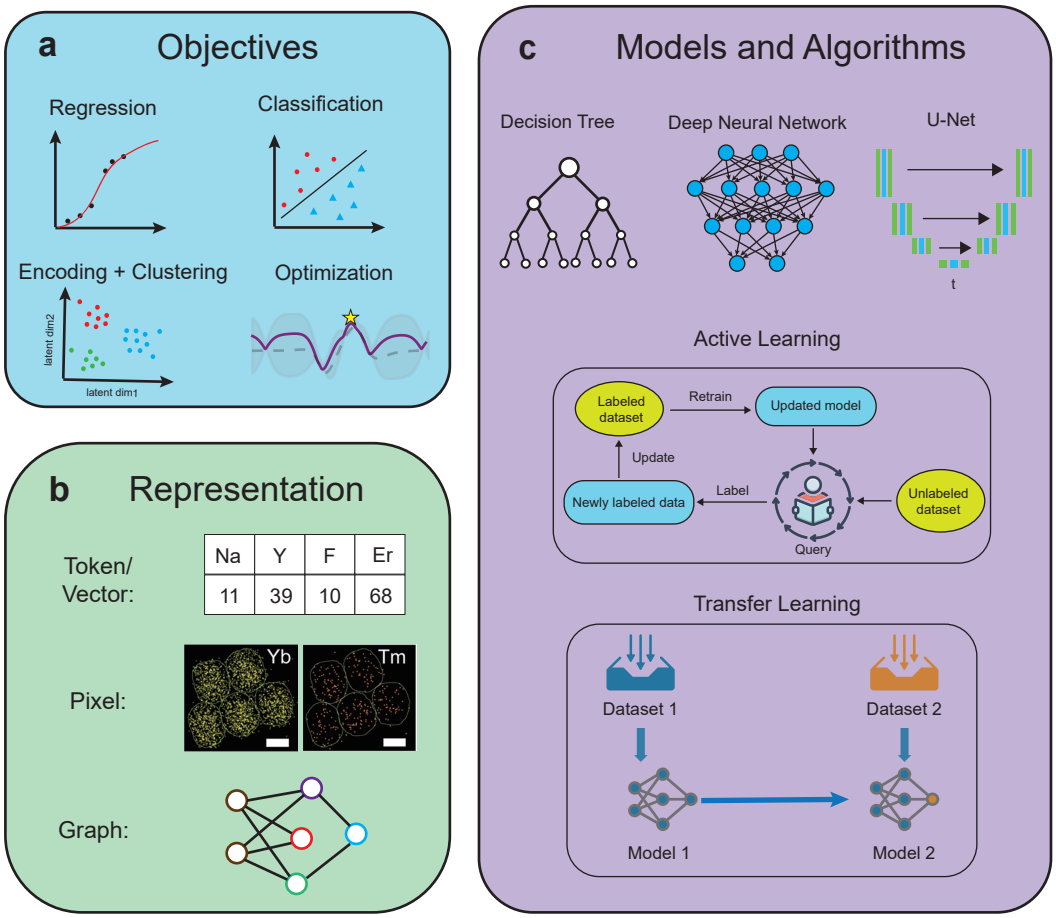

Figure 2. Examples of ML objectives (a), data representations (b), and models/architectures (c). Scanning transmission electron microscopy images in (b) were reproduced from Ruan and Zhang.[76]

3. Machine learning

To understand how to apply ML to UCNPs, we must identify the four major components of an ML problem: the Objective, Data, Representation, and Model (Figure 2). These components define, respectively, the goal or metric to achieve (Figure 2a), the evidence on which to learn, the method for digitally encoding the materials (Figure 2b), and the algorithm used to learn and generalize (Figure 2c). As we discuss below, ML models range from simple regressors to deep neural networks, from models trained by labeled data to unsupervised models, and from models that guide experiments autonomously to those that generate new materials to test.

Surrogate models for supervised learning. A major bottleneck in UCNP research is that experiments and high-fidelity simulations are costly, limiting the rate of materials discovery and property optimization. In a realistic materials design problem, the mapping from the structure to its properties is often highly nonlinear and noisy. Surrogate models approximate this mapping with a more computationally efficient substitute in the form of a function $y = f(x)$, where x is a collection of features (e.g., a vector of dopant concentrations or shell diameters) and y is a collection of observed properties (*e.g.,* the UCNP spectrum or brightness). $f(x)$ varies with x and parameters that are fit using existing data (y) that is labeled by the features (x) of those materials – a process known as supervised learning. After

the surrogate model $f(x)$ is trained with such labeled data, the model can be used to evaluate untested structures. This forward process, known as inference, provides fast property estimates, enabling inexpensive screening and iterative optimization at scale.[77, 78]

Surrogate modeling tasks are typically formulated as regression or classification (Figure 2a). Regression models predict continuous-valued properties (e.g., band gap, elastic modulus, emission intensity, decay lifetime), whereas classification models predict discrete labels (e.g., crystal quality[54, 79] or phase,[55] metal/insulator, paramagnetic/ferromagnetic). Surrogate models (Figure 2c) range from classical machine-learning algorithms – such as Gaussian Process Regression, Support Vector Regression,[79] and tree-based ensembles (e.g., Random Forest) – to modern deep learning (DL) approaches that use artificial neural networks with many layers to approximate high-dimensional functions. For complex materials like UCNPs, whose structure is not easily described by a list (vector) of known features, DL models can operate on richer data modalities such as images and graphs.[4] Model architecture (Figure 2c) is often chosen to match the data type (Figure 2b): multilayer perceptrons are effective for fixed-length feature vectors; convolutional neural networks (CNNs) are well suited for microstructure images; and graph neural networks (GNNs) provide a natural framework for atomistic structures and highly interconnected relationships.

Unsupervised learning. Whereas supervised learning with surrogate models requires the time-consuming labeling of many (x,y) data pairs, unsupervised ML models have been developed to operate only on input data (y) without explicit labels (x). Rather than mapping structure to property, unsupervised methods seek to uncover latent (hidden) structure in the data, for example by grouping samples with similar behavior (e.g., UCNPs that exhibit pure red emission with high quantum yield) or describing the variation in the dataset with fewer variables than the input dataset (e.g., by identifying common spectral components). Typical unsupervised techniques include dimensionality reduction, such as principal component analysis (PCA[80]), and clustering methods such as k-means, which partitions data into groups based on similarity (Figure 2a). These approaches are used to organize large composition or structure spaces, identify families of materials with similar behavior, and detect outliers or mislabeled samples. Unsupervised models do not intrinsically know that the UCNPs in a red-emitting cluster are codoped with Er^{3+} and Tm^{3+} or Ho^{3+}, but those clusters can prompt further studies that reveal such correlation. Unsupervised learning also underpins modern generative AI for materials: unconditional generative models such as variational autoencoders, generative adversarial networks (GANs), and diffusion models learn the underlying distribution over compositions or structures and can sample novel candidate materials, much like such models can generate new human faces from existing photographs. Generated structures can then be guided or filtered by supervised surrogate models and physical constraints to accelerate materials discovery.

Sequential learning. While supervised and unsupervised models are often trained by fitting them simultaneously on a single dataset, sequential learning algorithms learn incrementally from a series of experiments, selecting which ones to perform in each iteration. Data from one set of experiments is used to retrain an underlying surrogate model, which is then used by the algorithm to select the next set of experiments. This results in a closed feedback loop that is repeated continually to optimize a quantifiable material property (known as the objective function) while reducing the amount of data needed to train the surrogate model.[81] For example, active learning[55, 82] (Figure 2c) iteratively optimizes model performance (e.g., accuracy) by selecting informative new samples, such as those in underexplored regions where the model has high uncertainty or those expected to most improve the model. Meanwhile, Bayesian optimization (Figure 4a) optimizes model performance and material properties simultaneously, and is ideal when budgets are small and evaluations are expensive.[3, 58, 83, 84] In contrast, reinforcement learning[85] (RL) learns a policy for making decisions under a given set of conditions so as to maximize some

ultimate objective. Such approaches are valuable for dynamic tuning of serial, path-dependent processes such as UCNP growth or assembly to maximize optical properties or structural order.[86]

A key limitation of many ML models is that they are trained for specific systems and may struggle to generalize to new materials or extrapolate to new conditions. Techniques such as transfer learning[87] (Figure 2c) and fine-tuning have been developed to adapt pretrained models to new and related tasks while reducing the amount of additional training. Active meta-learning uses an ensemble of historical models trained on different tasks (e.g., optimizing the growth of perovskites with different cations[79, 88]) to train a meta-model optimized for learning future tasks (e.g., growth with new cations) with only a few additional experiments.[89] While many other ML models exist, this brief introduction demonstrates the broad capabilities of ML that can be applied to UCNP design, synthesis, and characterization.

4. Applications of ML to UCNPs

While data-driven methods based on physical models and automated synthesis have been used extensively to explore UCNP structure and properties, the actual application of ML and modern deep learning architectures to UCNP research only emerged recently, in 2020, and is still limited to a handful of examples discussed below. This relative scarcity may be due to the dearth of large, high-quality, standardized datasets and meaningful ML representations that capture the structural and photophysical complexity of UCNPs. Nevertheless, we can gain insight from the more extensive library of AI approaches used to explore bulk upconverting materials and lanthanide complexes, as well as to optimize nanoparticles for downshifting and downconversion applications.[90]

ML for raw data analysis. The most prevalent application of ML to UCNPs has been to accelerate the processing of raw characterization data such as microscope images and luminescence spectra. These models leverage existing ML architectures for image analysis, denoising, and pattern matching. For example, Wen et al.[91] used unsupervised clustering to automate UCNP sizing from transmission electron microscopy (TEM) images, enabling objective, statistically representative analysis (Figure 3a). In parallel, data-driven models have been employed to analyze time-resolved luminescence signals from UCNPs. Liao et al.[92] used a CNN to automate the decoding of complex lifetime fingerprints from single UCNPs and resolve overlapping signals (Figure 3b). Similarly, Liu et al.[93] used neural networks to analyze the lifetimes of single UCNPs in super-resolution imaging, successfully identifying densely clustered particles with over 93% accuracy. More recently, deep-learning-based image reconstruction architectures have been explored to extract data from images[94] and convert low-quality raw signals into higher-fidelity outputs.[93, 95] Wu et al.[96] employed a CycleGAN model trained on UCNP images measured at two different emission wavelengths (455 and 808 nm) to enhance the resolution at longer wavelengths in highly scattering specimens (Figure 3c). These examples demonstrate that ML can rapidly extract critical physical parameters from UCNP characterization, enabling efficient processing of large, high-dimensional datasets and samples from high-throughput experimental workflows.

ML for application-specific interpretation of data. Beyond aiding raw data analysis, ML models have been extended to applications more specific to UCNPs and lanthanide-doped nanocrystals, such as using the luminescence of the lanthanide ions to infer the environment surrounding the nanoparticle probes.[97, 98] Although using downshifting instead of upconversion, Ximendes et al,[99] Santos et al,[100] and others have leveraged automated ML-based analysis of emission spectra to perform more accurate and precise real-time temperature measurements within rare-earth-doped nanoparticles. Here, ML directly infers meaningful patterns or quantitative metrics from optical signals within an application context,

rather than extracting physical data, which is beneficial due to the complex and non-linear relationship between UCNP luminescence and external stimuli.

ML has been particularly prevalent in the biomedical applications of UCNPs, making logical decisions or evaluations from the results of UCNP-based biomedical assays. Mejia-Mendez et al.[97] trained eight different ML models to predict cell viability in the presence of Yb^{3+}/Er^{3+}-doped ZnO UCNPs using inputs including particle size, concentration, and composition, host matrix band structure, and cell type. ML models have also been used to map the transient signals of UCNP-based immunoassay devices to blood drug concentrations for real-time pharmacokinetic monitoring.[98] Furthermore, Zhai et al.[101] utilized a CNN to rapidly quantify gallic acid concentrations from colorimetric and luminescent features in smartphone images of UCNP test strips. After extracting the spatiotemporally varying positions of UCNP-tagged motor proteins from upconversion micrographs, Yi et al.[102] used these trajectories as inputs to train a Support Vector Machine (SVM) that classifies the neurotoxicity of drugs (Figure 3d).

In information technology, ML-based pattern recognition has been applied to optical encryption, facilitating the decryption of 188 distinct fingerprints encoded in the time-dependent luminescence of pulse-modulated UCNPs.[103] In an interesting inversion, UCNPs have also been used as the physical hardware to execute ML operations[104] and construct physical neural networks.[105] Bednarkiewicz et al.[36] leveraged the long lifetimes and extreme nonlinearity of photon avalanching nanoparticles (ANPs) to perform optical reservoir computing in what could be considered a random optical neural network. The Tm^{3+} $4f^{12}$ states in ANPs act as information reservoirs that integrate multiple signals in a non-additive fashion, enabling classification of numeric digits whose images are represented as a series of excitation light pulses.[36] Just as nonlinear activation layers enable artificial neural networks to model complex data, the nonlinearity of ANPs is critical for capturing complex spatial information needed for accurate image recognition. The authors also classified the digits by feeding the ANP-encoded signals into a 2-layer NN, illustrating that ANPs can be used as embedding layers (i.e., reducing dimensionality) for ML models.

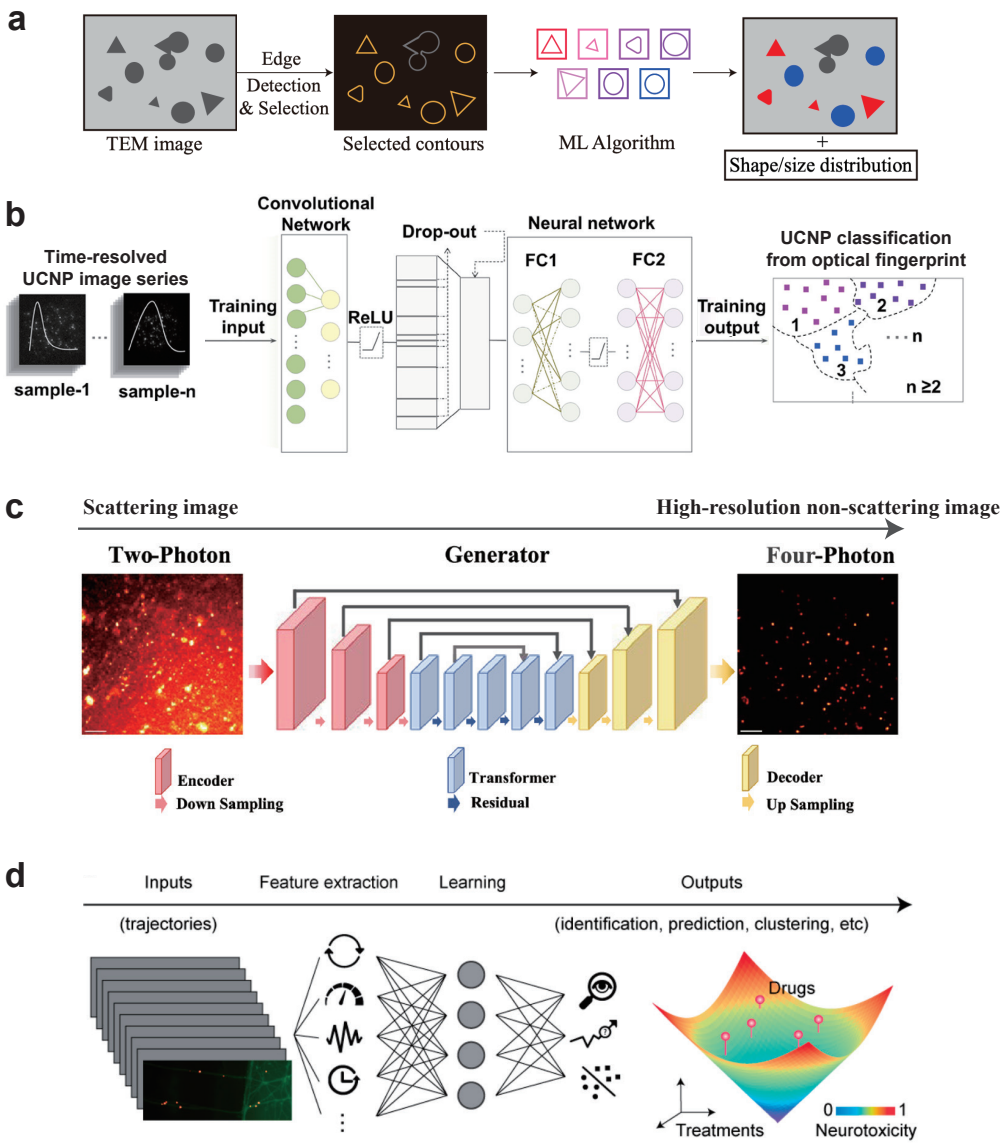

Figure 3. Examples of ML in UCNP Research. (a) Unsupervised clustering for automated TEM image processing by Wen et al.[91] (b) CNN for classifying single UCNP lifetime decay curves for high-capacity optical multiplexing. Adapted with permission from Liao et al.[92] Copyright 2021 American Chemical Society. (c) Generative adversarial network (CycleGAN) upscaling low-resolution 2-photon upconversion micrographs into high-resolution, 4-photon-equivalent images for deep-tissue bio-imaging. Reproduced from Wu et al.[106] (d) SVM predicting drug-induced neurotoxicity from intraneural UCNP trajectories. Reproduced with permission from Yi et al.[102] Copyright 2021 American Chemical Society.

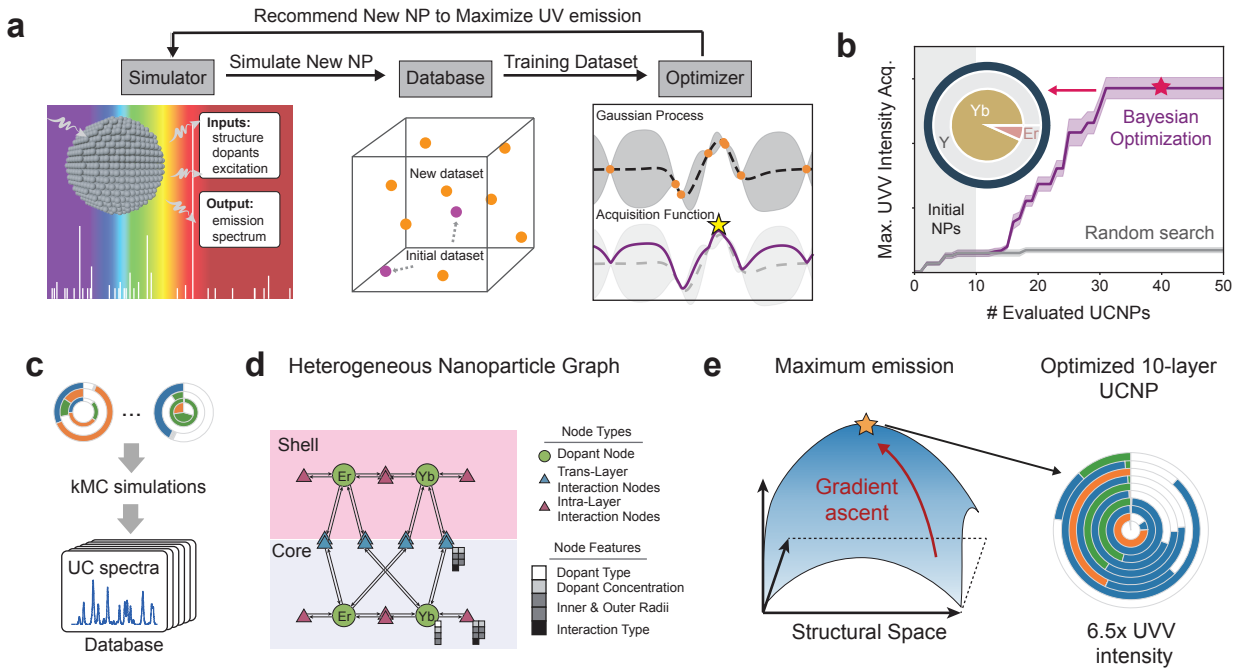

Figure 4. ML applications in UCNP inverse design. (a) Bayesian optimization workflow for simulating emission spectra (left) with kinetic Monte Carlo (kMC) given an input UCNP structure, composition, and excitation parameters. Schematic illustration of design space exploration (middle) during the optimization. Bayesian optimization algorithm (right) based on Gaussian Process to evaluate the acquisition during the iteration. (b) Optimization performance of a Yb^{3+}/Er^{3+}-doped $NaYF_4$ UCNP recommended by the BO workflow (purple line) and random search (gray line). (a), (b) Reprinted with permission from Xia et al.[3] Copyright 2023 American Chemical Society. (c) Generation of SUNSET database of UCNP spectra simulated by kMC simulations. (d) Heterogeneous graph representation of a UCNP. (e) Gradient-based search in UCNP structural design using the hetero-GNN surrogate model based on the graph representation in (d). (c), (d), and (e) Reproduced from Sivonxay et al.[4]

ML for evaluating and optimizing UCNP structures. While ML has accelerated the processing of UCNP luminescence data, there are few examples utilizing AI to design and discover new UCNP compositions or structures.[107] In one example, Bao et al.[108] used literature data to train eight different ML regression models to predict the thermally induced upconversion luminescence enhancement from structural features of Er^{3+}/Yb^{3+} co-doped UCNPs, including dopant concentrations, host phonon energy, absorption cross-section, and particle morphology. The authors found that combining the different models into an ensemble model provided the highest predictive accuracy.

UCNP research is only beginning to exploit sequential learning to optimize UCNP structure and properties. One of the first such applications was our active learning of core/shell UCNPs using Bayesian optimization (BO) with Gaussian processes (GPs).[3] A GP surrogate model trained on kMC data learned a probabilistic mapping of UCNP structure (e.g., core and shell radii) and composition to targeted properties – in this case, the simulated UV-violet emission (UVV, 300-450 nm). An acquisition function leveraged the model's predicted mean and uncertainty to propose the next candidate for kMC simulation. By repeatedly cycling through kMC evaluation and model refinement in a closed-loop computational pipeline (Figure

4a), the workflow rapidly optimized heterostructures, delivering ca. 10-fold UVV enhancement for Yb^{3+}/Er^{3+}-codoped UCNPs within 22 BO iterations (Figure 4b) and ca. 110-fold enhancement for $Yb^{3+}/Er^{3+}/Tm^{3+}$ triply doped UCNPs after 40 iterations.[3] Notably, the BO pipeline was able to autonomously navigate heterostructure design space and learn well-established UCNP design principles (e.g., highly doped cores combined with inert shells promote upconversion), 500 times faster than the historical rate of discovery.

Heterogeneous GNN surrogates for differentiable inverse design. While BO can efficiently explore simple systems such as core-shell nanoparticles, it is well known that BO becomes computationally intractable with large numbers of features,[109] which is the case for complex UCNP heterostructures with multiple shells and dopants.[46] In addition, simulating such large, multi-component UCNPs also becomes prohibitively slow – some kMC simulations take more than two months on high-performance computing clusters, severely limiting exploration in high-dimensional combinatorial design space. As an alternative, we explored deep-learning surrogate models, which can model complex, high dimensional spaces and rapidly approximate physical properties (e.g., emission intensity). A central challenge, however, lies in how to represent UCNPs in DL models. Nanomaterials often exhibit properties distinct from their bulk counterparts, yet their structures are too complex for conventional vector representations and difficult to describe with hand-crafted descriptors.

To address these scaling and representation challenges for complex multi-shell UCNPs, we developed a graph-based inverse design approach that replaces expensive kMC simulations with deep GNNs and BO with gradient-based optimization (Figure 4cde).[4] Graph representations (Figure 2b) are a natural fit for materials[110] such as UCNPs because each node (circle) can contain features of different types (e.g., elemental identity, local coordination environment), while the edges connecting the nodes represent relationships between those nodes – interactions that can be conditioned by factors such as distance or rate. These characteristics are essential for UCNPs due to their dependence on nonlinear ET interactions and their wide variety of features. Moreover, graphs efficiently encode UCNP features across a broad range of length scales, from atomic interactions to >100 nm UCNP diameters, which is impractical using image-based representations. We developed UCNP graph representations in which dopant nodes (green circles in Figure 4d) represent the different types of dopants in a given domain (e.g., Er^{3+} dopants in the UCNP core), with node features encoding dopant identity, concentration, and geometric information. Critically, we found that representing the different ET interactions (e.g., core $Er^{3+}\rightarrow$ shell Yb^{3+} ET) as a second type of node (triangles in Figure 4d), rather than as edges, maximized the accuracy of our GNN by allowing more information, such as interaction type and distance, to be passed as messages between the dopant nodes during model training and inference.

To predict emission intensity directly from UCNP heterostructure designs, we trained a GNN based on our heterogeneous graph representation (hetero-GNN) with a dataset of >6,000 UCNP spectra[4] (SUNSET, Figure 4c) that we simulated with kMC.[74] Compared to different baseline models and representations (e.g., image-based CNNs), the hetero-GNN achieved the lowest prediction error. Notably, the hetero-GNN exhibited more accurate extrapolation to UCNP structures far outside of the training set distribution, e.g., UCNPs with four shells vs. training set UCNPs with up to 3 shells. Crucially, the surrogate is differentiable, allowing us to use the hetero-GNN model with common gradient-based optimizers for rapid inverse design. Using basin-hopping–style global search on the trained hetero-GNN, we optimized UCNP heterostructures with up to 9 shells to have 6.5-fold greater predicted UVV emission than the highest intensity in the training set (Figure 4e).[4]

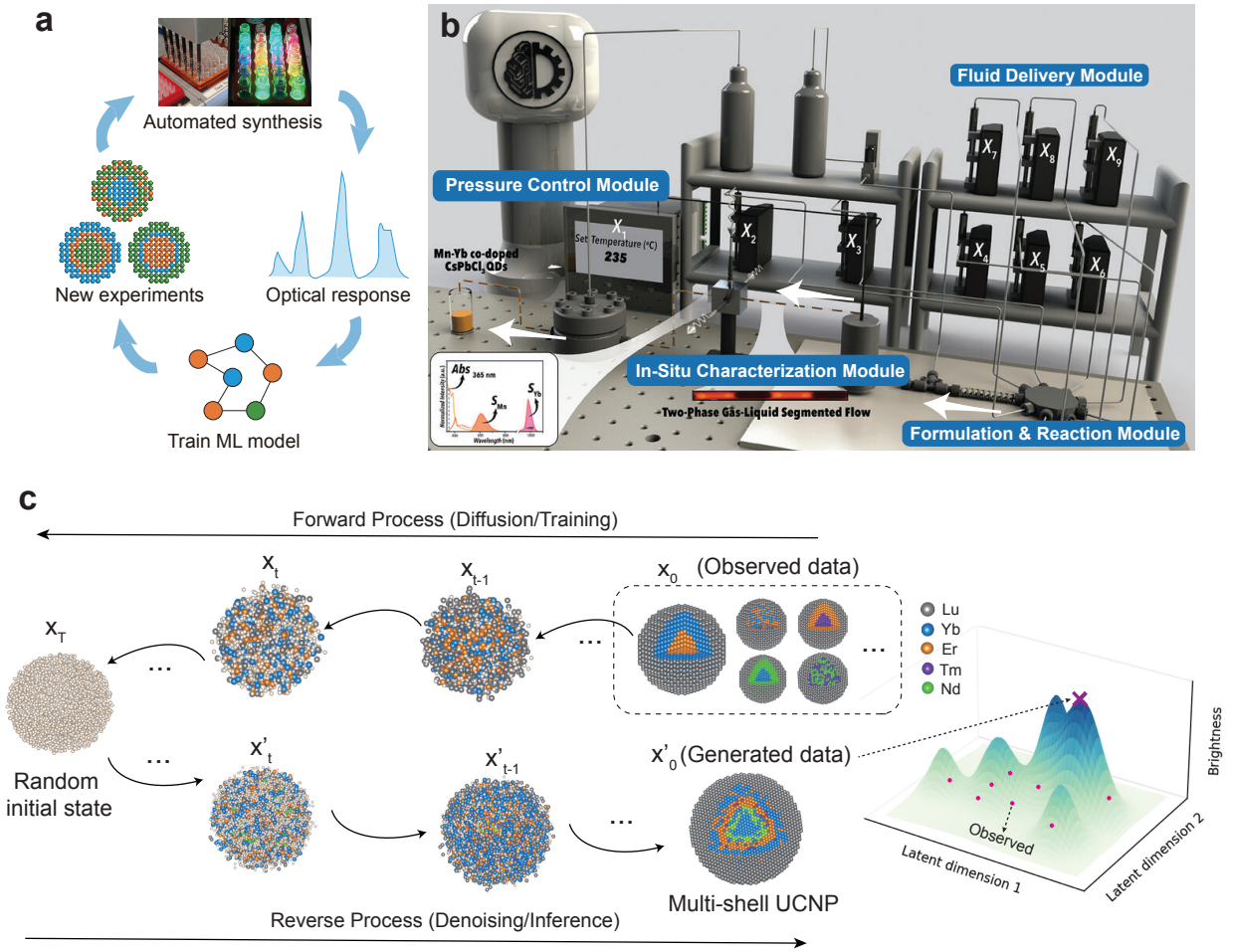

Figure 5. Future applications of ML to UCNPs. (a) ML-guided autonomous synthesis of UCNPs. (b) Smart Dope autonomous flow chemistry platform for optimizing downconversion in Mn^{2+}/Yb^{3+}-doped $CsPbCl_3$ nanoparticles. Reproduced from Bateni et al.[58] (c) DDPM-based generative AI model for novel core-shell nanoparticle design.

5. Future applications of ML to UCNP research

As the application of ML-assisted UCNP research progresses, ML will become more deeply integrated into UCNP research, just as AI has become increasingly present in modern technology. Future UCNP research will fully embrace recent progress in autonomous experimentation, generative AI, and large language models, as discussed below.

Autonomous synthesis of UCNPs. Although we have previously demonstrated automated robotic synthesis of UCNPs and ML-guided computational optimization of UCNP heterostructures, there is little work integrating AI directly into the decision making of automated experimental workflows to discover new UCNP structures in an unattended manner. In such autonomous workflows, or Self-Driving Laboratories (SDLs),[56] an ML agent suggests experiments to perform based on historical data, initiates automated synthesis and subsequent characterization of the products, uses the new experimental data

to update the ML model, which is then used to recommend the next series of experiments (Figure 5a). Such "closed-loop" workflows have the potential to dramatically accelerate the discovery of new UCNPs due to their ability to intelligently explore ultrahigh-dimensional spaces that elude human intuition and biases.

SDLs based on microfluidics, laboratory automation robots, and mobile robots, have already been developed for photocatalysts,[111] photovoltaic materials,[112] organic dyes for lasing,[113] chiral nanoparticles,[64] and semiconductor nanocrystal heterostructures.[67] To discover Mn^{2+}/Yb^{3+}-codoped $CsPbCl_3$ nanocrystals for "quantum cutting," Abolhasani et al.[58] integrated ensemble neural networks and BO with an autonomous flow-chemistry platform named "Smart Dope" (Figure 5b) to identify compositions with downconversion luminescence quantum yields as high as 158%.

UCNPs represent an attractive platform for such autonomous frameworks, with their intricate, high-dimensional design space and complex, non-linear optical responses. However, this high-dimensionality also presents a challenge to SDLs since it requires far larger datasets than can be produced experimentally, and far larger numbers of iterations that can be performed in a reasonable timeframe. SDLs for UCNPs (Figure 5a) could adopt a more integrative autonomous strategy in which experimental data is supplemented with computational modeling of various fidelities[114] and with literature data parsed by large language models. Such a multifidelity integrated approach reduces the need for large quantities of expensive experimental data and would provide a robust and scalable foundation for navigating the inherent complexity of lanthanide-doped nanomaterials.

Generative AI for UCNP design. Autonomous UCNP discovery requires a method to computationally generate hypotheses and new lanthanide-doped structures to test, particularly materials predicted to have targeted properties like brightness in selected spectral windows, nonlinearity, and switching behavior. Despite our progress in computationally predicting optical properties from UCNP structure, performing the inverse operation – predicting a UCNP structure that will have a defined set of properties – is still challenging. One reason is that AI tools such as regression models have excelled at refining material designs by interpolating within existing structure templates and heuristics, but they have struggled to extrapolate beyond their training data. This means that such models are less likely to explore qualitatively new structural motifs or counter-intuitive configurations – precisely the kinds of designs needed to achieve order-of-magnitude gains in UCNP performance rather than incremental improvements.

We anticipate that UCNP research will increasingly adopt generative AI (GenAI) approaches to propose novel candidate UCNP structures. GenAI methods are already being exploited in materials: diffusion-based models such as MatterGen[115] demonstrate that one can generate stable inorganic crystals and perform crystal structure prediction (CSP) by sampling structures conditioned on composition and properties. A denoising diffusion probabilistic model (DDPM) could be trained to generate new multi-shell UCNPs (Figure 5c) by first using a forward process to gradually perturb observed UCNP structures with Gaussian noise, while a neural denoiser such as a time-conditioned U-Net CNN (Figure 2c) learns to predict the noise added at each step *t*. The reverse denoising process can then be used to generate novel UCNP heterostructures. Similar generative frameworks in synthesis design[116] use learned reaction models to propose chemically plausible reaction pathways that achieve a target product.

The key difference from mainstream UCNP optimization is that methods like BO or gradient-based refinement propose candidates by navigating a landscape, whereas GenAI can generate diverse candidates that meet desired targets (spectral features, brightness, lifetime, and synthesizability). These

target families are spread over the distribution of possible UCNP structures, naturally reflecting the multi-modal nature of UCNP inverse maps – different architectures can realize similar outputs via different pathway balances. This is especially valuable for UCNPs because we want not just the best predicted structure, but a set of alternatives that balance brightness vs. lifetime vs. spectra – under certain hard constraints (e.g., minimum shell thickness, bounded dopant loading, allowed layer sequences). Looking forward, the most promising roadmap is therefore a stack: advanced representations (e.g., graph/heterogeneous-graph descriptions of layered domains and dopant interactions), rich datasets (large-scale kMC and rate-equation simulations, plus high-throughput experimental data), and physics-inspired generative algorithms. RL can further bias or fine-tune the generator toward candidates with maximal predicted reward (e.g., emission intensity, favorable ET pathways), in close analogy to emerging diffusion+RL frameworks in molecular design and synthesis planning.

Large language models (LLMs) are another class of generative AI that promise to enhance UCNP research.[117] Already used for the discovery of extractants that separate lanthanides,[117] LLMs prompted by informal queries could be used to aggregate and summarize UCNP data from diverse sources, including literature, experimental databases, and unstructured notebooks. More significantly, LLMs could be used to generate hypotheses[118] and detailed experimental plans[119] that could direct autonomous experimental workflows. Although they did not investigate upconversion, Schaak et al[73] used an LLM trained on their high-throughput dataset of robotically synthesized lanthanide-doped nanoparticle heterostructures to identify and autonomously synthesize nanoparticles with 1-4 rare earth elements that met specified constraints.

Key considerations for all LLMs and deep learning approaches are the large quantity of reliable data needed to train such models, as well as user- and application-programming interfaces to efficiently access such data.[88] Unlike fields such as biology, where contribution to public databases is normalized and even required, there are few databases of well-labeled UCNP data.[4] In order to reach the influence of models such as AlphaFold,[120] the UCNP community must collectively agree to deposit data and metadata (e.g., experimental parameters) in shared databases using standardized formats and FAIR (Findable, Accessible, Interoperable, Reusable) data principles.[121]

6. Conclusion

Although UCNP research is only beginning to utilize ML, the applications surveyed here strongly suggest that ML can and will enhance UCNP research in the future. The adoption of ML-guided approaches will almost certainly expand until it becomes mundane and indistinguishable from everyday UCNP science. However, advances in the areas of hypothesis generation, physics-informed models, extrapolation far outside training data, and physical interpretation of ML models are needed before AI-guided approaches can challenge human intuition, creativity, and understanding. We predict that AI-based techniques will primarily be used to enhance human experimentation, with cutting-edge discoveries like ANPs still requiring human intervention and improvisation. Considering how AI has already changed science, from predicting protein structures[120] to analyzing massive material datasets,[53] it will be fascinating to see where ML takes UCNP research in the future.

Biographies

Ripeng Luo is a Materials Science and Engineering Ph.D. student at the University of California at Berkeley (UC-Berkeley). He received a M.S. in Materials Science from Tsinghua University. His interests include AI-assisted materials discovery. He works with Dr. Emory Chan on advanced ML methods and theory-guided autonomous synthesis workflows for closed-loop UCNP design.

Jungmin Hamm is a postbaccalaureate researcher with Emory Chan in the Molecular Foundry at Lawrence Berkeley National Laboratory (LBNL). He received a B.S. in Chemistry from Sogang University. His interests include the development of robotic platforms that facilitate ML-guided discovery.

Emory Chan is a Staff Scientist at the Molecular Foundry, LBNL. He received a B.S. in Chemistry from Stanford University and a Ph.D. in Chemistry from UC-Berkeley. He investigates nanomaterials with complex compositions, such as UCNPs, and their complex ET networks, using high-throughput approaches including robotic workflows that enable ML-guided experimentation.

Acknowledgements
The authors thank S. Blau, E. Sivonxay, and X. Xia for performing and inspiring much of the ML UCNP work discussed in this Account. Work at the Molecular Foundry was supported by the Office of Science, Office of Basic Energy Sciences, of the U.S. Department of Energy under Contract No. DE-AC02-05CH11231, under proposal number MFP-10241 and under the Laboratory Directed Research and Development program of LBNL.

Notes

The authors declare no competing financial interest.

References

(1) Chan, E. M.; Han, G.; Goldberg, J. D.; Gargas, D. J.; Ostrowski, A. D.; Schuck, P. J.; Cohen, B. E.; Milliron, D. J. Combinatorial Discovery of Lanthanide-Doped Nanocrystals with Spectrally Pure Upconverted Emission. *Nano Lett.* **2012**, *12* (7), 3839-3845.
(2) Qi, X.; Lee, C.; Ursprung, B.; Skripka, A.; Schuck, P. J.; Chan, E. M.; Cohen, B. E. Short-Wave Infrared Upconverting Nanoparticles. *Journal of the American Chemical Society* **2024**, *146* (43), 29292-29296.
(3) Xia, X.; Sivonxay, E.; Helms, B. A.; Blau, S. M.; Chan, E. M. Accelerating the Design of Multishell Upconverting Nanoparticles through Bayesian Optimization. *Nano Lett.* **2023**, *23* (23), 11129-11136.
(4) Sivonxay, E.; Attia, L.; Spotte-Smith, E. W. C.; Sanchez-Lengeling, B.; Xia, X.; Barter, D.; Chan, E. M.; Blau, S. M. Gradient-based optimization of complex nanoparticle heterostructures enabled by deep learning on heterogeneous graphs. *Nature Computational Science* **2026**, *6* (1), 83-95.
(5) Qi, X.; Ercius, P.; Schuck, P. J.; Cohen, B. E.; Chan, E. M. Synthetic Control over the Electron-Beam Stability of Upconverting Nanoparticles. *Nano Lett.* **2026**, *2026*, in press.
(6) Chen, G.; Qiu, H.; Prasad, P. N.; Chen, X. Upconversion Nanoparticles: Design, Nanochemistry, and Applications in Theranostics. *Chem. Rev.* **2014**, *114* (10), 5161-5214.
(7) Chan, E. M. Combinatorial approaches for developing upconverting nanomaterials: high-throughput screening, modeling, and applications. *Chem. Soc. Rev.* **2015**, *44* (6), 1653-1679, 10.1039/C4CS00205A.
(8) Pan, J. A.; Qi, X.; Chan, E. M. Enhanced upconversion and photoconductive nanocomposites of lanthanide-doped nanoparticles functionalized with low-vibrational-energy inorganic ligands. *Nanoscale Horizons* **2025**, *10* (3), 596-604, 10.1039/D4NH00555D.
(9) Ma, Y.; Chen, Y.; Wang, S.; Chen, Z.-H.; Zhang, Y.; Huang, L.; Zhang, X.; Yin, F.; Wang, Y.; Yang, M.; et al. Near-infrared spatiotemporal color vision in humans enabled by upconversion contact lenses. *Cell* **2025**, *188* (13), 3375-3388.e3318.
(10) Wu, X.; Zhang, Y.; Takle, K.; Bilsel, O.; Li, Z.; Lee, H.; Zhang, Z.; Li, D.; Fan, W.; Duan, C.; et al. Dye-Sensitized Core/Active Shell Upconversion Nanoparticles for Optogenetics and Bioimaging Applications. *ACS Nano* **2016**, *10* (1), 1060-1066.
(11) Chen, S.; Weitemier, A. Z.; Zeng, X.; He, L.; Wang, X.; Tao, Y.; Huang, A. J. Y.; Hashimotodani, Y.; Kano, M.; Iwasaki, H.; et al. Near-infrared deep brain stimulation via upconversion nanoparticle–mediated optogenetics. *Science* **2018**, *359* (6376), 679, 10.1126/science.aaq1144.
(12) Liu, H.; Ju, Z.; Hui, X.; Li, W.; Lv, R. Upconversion and NIR-II luminescent rare earth nanoparticles combined with machine learning for cancer theranostics. *Nanoscale* **2024**, *16* (35), 16697-16705, 10.1039/D4NR01861C.
(13) Evans, M. A.; Huang, P.-J.; Iwamoto, Y.; Ibsen, K.; Chan, E. M.; Hitomi, Y.; Ford, P. C.; Mitragotri, S. Macrophage-mediated delivery of light activated nitric oxide prodrugs with spatial, temporal and concentration control. *Chemical Science* **2018**, *9* (15), 3729-3741, 10.1039/C8SC00015H.
(14) Punjabi, A.; Wu, X.; Tokatli-Apollon, A.; El-Rifai, M.; Lee, H.; Zhang, Y.; Wang, C.; Liu, Z.; Chan, E. M.; Duan, C.; et al. Amplifying the red-emission of upconverting nanoparticles for biocompatible clinically used prodrug-induced photodynamic therapy. *ACS Nano* **2014**, *8* (10), 10621-10630.
(15) Idris, N. M.; Gnanasammandhan, M. K.; Zhang, J.; Ho, P. C.; Mahendran, R.; Zhang, Y. In vivo photodynamic therapy using upconversion nanoparticles as remote-controlled nanotransducers. *Nat. Med.* **2012**, *18*, 1580.
(16) Pan, J.-A.; Skripka, A.; Lee, C.; Qi, X.; Pham, A. L.; Woods, J. J.; Abergel, R. J.; Schuck, P. J.; Cohen, B. E.; Chan, E. M. Ligand-Assisted Direct Lithography of Upconverting and Avalanching Nanoparticles for Nonlinear Photonics. *Journal of the American Chemical Society* **2024**, *146* (11), 7487-7497.
(17) Wu, S.; Han, G.; Milliron, D. J.; Aloni, S.; Altoe, V.; Talapin, D. V.; Cohen, B. E.; Schuck, P. J. Non-blinking and photostable upconverted luminescence from single lanthanide-doped nanocrystals. *Proc. Natl. Acad. Sci. U. S. A.* **2009**, *106* (27), 10917-10921.
(18) Nam, S. H.; Bae, Y. M.; Park, Y. I.; Kim, J. H.; Kim, H. M.; Choi, J. S.; Lee, K. T.; Hyeon, T.; Suh, Y. D. Long-Term Real-Time Tracking of Lanthanide Ion Doped Upconverting Nanoparticles in Living Cells. *Angewandte Chemie Int. Ed. Eng.* **2011**, 6093-6097.
(19) Ostrowski, A. D.; Chan, E. M.; Gargas, D. J.; Katz, E. M.; Han, G.; Schuck, P. J.; Milliron, D. J.; Cohen, B. E. Controlled Synthesis and Single-Particle Imaging of Bright, Sub-10 nm Lanthanide-Doped Upconverting Nanocrystals. *ACS Nano* **2012**, *6* (3), 2686-2692.
(20) Gargas, D. J.; Chan, E. M.; Ostrowski, A. D.; Aloni, S.; Altoe, M. V. P.; Barnard, E. S.; Sanii, B.; Urban, J. J.; Milliron, D. J.; Cohen, B. E.; et al. Engineering bright sub-10-nm upconverting nanocrystals for single-molecule imaging. *Nat. Nanotechnol.* **2014**, *9*, 300.
(21) Fardian-Melamed, N.; Skripka, A.; Ursprung, B.; Lee, C.; Darlington, T. P.; Teitelboim, A.; Qi, X.; Wang, M.; Gerton, J. M.; Cohen, B. E.; et al. Infrared nanosensors of piconewton to micronewton forces. *Nature* **2025**, *637* (8044), 70-75.
(22) Bednarkiewicz, A.; Chan, E. M.; Prorok, K. Enhancing FRET biosensing beyond 10 nm with photon avalanche nanoparticles. *Nanoscale Advances* **2020**, *2* (10), 4863-4872, 10.1039/D0NA00404A.
(23) Tajon, C. A.; Yang, H.; Tian, B.; Tian, Y.; Ercius, P.; Schuck, P. J.; Chan, E. M.; Cohen, B. E. Photostable and efficient upconverting nanocrystal-based chemical sensors. *Opt. Mater.* **2018**, *84*, 345-353.
(24) Kilbane, J. D.; Chan, E. M.; Monachon, C.; Borys, N. J.; Levy, E. S.; Pickel, A. D.; Urban, J. J.; Schuck, P. J.; Dames, C. Far-field optical nanothermometry using individual sub-50 nm upconverting nanoparticles. *Nanoscale* **2016**, *8* (22), 11611-11616, 10.1039/c3cs60102a.
(25) Fernandez-Bravo, A.; Yao, K.; Barnard, E. S.; Borys, N. J.; Levy, E. S.; Tian, B.; Tajon, C. A.; Moretti, L.; Altoe, M. V.; Aloni, S.; et al. Continuous-wave upconverting nanoparticle microlasers. *Nat. Nanotechnol.* **2018**, *13*, 572–577.
(26) Fernandez-Bravo, A.; Wang, D.; Barnard, E. S.; Teitelboim, A.; Tajon, C.; Guan, J.; Schatz, G. C.; Cohen, B. E.; Chan, E. M.; Schuck, P. J.; et al. Ultralow-threshold, continuous-wave upconverting lasing from subwavelength plasmons. *Nat. Mater.* **2019**, *18* (11), 1172-1176.
(27) Liu, Y.; Teitelboim, A.; Fernandez-Bravo, A.; Yao, K.; Altoe, M. V. P.; Aloni, S.; Zhang, C.; Cohen, B. E.; Schuck, P. J.; Chan, E. M. Controlled Assembly of Upconverting Nanoparticles for Low-Threshold Microlasers and Their Imaging in Scattering Media. *ACS Nano* **2020**, *14* (2), 1508-1519.
(28) Skripka, A.; Chan, E. M. Unraveling the myths and mysteries of photon avalanching nanoparticles. *Materials Horizons* **2025**, *12* (11), 3575-3597, 10.1039/D4MH01798F.
(29) Huang, J.; Wei, G.; Wei, H.; Zhou, B. Controlling Photon Avalanche Upconversion in Nanoparticles toward Frontier Applications. *ACS Applied Optical Materials* **2024**, *2* (9), 1841-1853.

(30) Lee, C.; Xu, E. Z.; Liu, Y.; Teitelboim, A.; Yao, K.; Fernandez-Bravo, A.; Kotulska, A. M.; Nam, S. H.; Suh, Y. D.; Bednarkiewicz, A.; et al. Giant nonlinear optical responses from photon-avalanching nanoparticles. *Nature* **2021**, *589* (7841), 230-235.
(31) Szalkowski, M.; Kotulska, A.; Dudek, M.; Korczak, Z.; Majak, M.; Marciniak, L.; Misiak, M.; Prorok, K.; Skripka, A.; Schuck, P. J.; et al. Advances in the photon avalanche luminescence of inorganic lanthanide-doped nanomaterials. *Chem. Soc. Rev.* **2025**, *54* (2), 983-1026.
(32) Passini, L. N.; Chan, E. M.; Cohen, B. E. Photon Avalanching Nanoparticles. *Acc. Chem. Res.* **2026**, *59* (7), 1170-1176.
(33) Lee, C.; Xu, E. Z.; Kwock, K. W. C.; Teitelboim, A.; Liu, Y.; Park, H. S.; Ursprung, B.; Ziffer, M. E.; Karube, Y.; Fardian-Melamed, N.; et al. Indefinite and bidirectional near-infrared nanocrystal photoswitching. *Nature* **2023**, *618* (7967), 951-958.
(34) Chen, J.; Liu, C.; Xi, S.; Tan, S.; He, Q.; Liang, L.; Liu, X. Optical nonlinearities in excess of 500 through sublattice reconstruction. *Nature* **2025**, *643* (8072), 669-674.
(35) Skripka, A.; Zhang, Z.; Qi, X.; Ursprung, B.; Ercius, P.; Cohen, B. E.; Schuck, P. J.; Jaque, D.; Chan, E. M. Intrinsic optical bistability of photon avalanching nanocrystals. *Nat. Photonics* **2025**, *19* (2), 212-218.
(36) Bednarkiewicz, A.; Szalkowski, M.; Majak, M.; Korczak, Z.; Misiak, M.; Maćkowski, S. All-Optical Data Processing with Photon Avalanching Nanocrystalline Photonic Synapse. *Adv. Mater.* **2023**, *35* (42), 2304390.
(37) Liu, X.; Jiang, C.; Chen, G. Brightening Upconversion Nanoparticles. *Acc. Chem. Res.* **2026**.
(38) Fischer, S.; Bronstein, N. D.; Swabeck, J. K.; Chan, E. M.; Alivisatos, A. P. Precise Tuning of Surface Quenching for Luminescence Enhancement in Core–Shell Lanthanide-Doped Nanocrystals. *Nano Lett.* **2016**, *16* (11), 7241-7247.
(39) Shen, J.; Chen, G.; Vu, A.-M.; Fan, W.; Bilsel, O. S.; Chang, C.-C.; Han, G. Engineering the Upconversion Nanoparticle Excitation Wavelength: Cascade Sensitization of Tri-doped Upconversion Colloidal Nanoparticles at 800 nm. *Adv. Opt. Mater.* **2013**, *1* (9), 644-650.
(40) Teitelboim, A.; Tian, B.; Garfield, D. J.; Fernandez-Bravo, A.; Gotlin, A. C.; Schuck, P. J.; Cohen, B. E.; Chan, E. M. Energy Transfer Networks within Upconverting Nanoparticles Are Complex Systems with Collective, Robust, and History-Dependent Dynamics. *J. Phys. Chem. C* **2019**, *123* (4), 2678-2689.
(41) Skripka, A. Heavy Halide Nanomaterials as Next-Generation Hosts for Lanthanide Upconversion. *Journal of the American Chemical Society* **2026**.
(42) Dong, H.; Sun, L.-D.; Yan, C.-H. Local Structure Engineering in Lanthanide-Doped Nanocrystals for Tunable Upconversion Emissions. *Journal of the American Chemical Society* **2021**, *143* (49), 20546-20561.
(43) Zhang, Z.; Skripka, A.; Dahl, J. C.; Dun, C.; Urban, J. J.; Jaque, D.; Schuck, P. J.; Cohen, B. E.; Chan, E. M. Tuning Phonon Energies in Lanthanide-doped Potassium Lead Halide Nanocrystals for Enhanced Nonlinearity and Upconversion. *Angew. Chem. Int. Ed.* **2023**, *62* (1), e202212549.
(44) Li, X.; Shen, D.; Yang, J.; Yao, C.; Che, R.; Zhang, F.; Zhao, D. Successive Layer-by-Layer Strategy for Multi-Shell Epitaxial Growth: Shell Thickness and Doping Position Dependence in Upconverting Optical Properties. *Chem. Mater.* **2013**, *25* (1), 106-112.
(45) Wang, F.; Deng, R.; Wang, J.; Wang, Q.; Han, Y.; Zhu, H.; Chen, X.; Liu, X. Tuning upconversion through energy migration in core–shell nanoparticles. *Nat. Mater.* **2011**, *10* (12), 968-973.
(46) Skripka, A.; Lee, M.; Qi, X.; Pan, J.-A.; Yang, H.; Lee, C.; Schuck, P. J.; Cohen, B. E.; Jaque, D.; Chan, E. M. A Generalized Approach to Photon Avalanche Upconversion in Luminescent Nanocrystals. *Nano Lett.* **2023**, *23* (15), 7100-7106.
(47) Xu, H.; Han, S.; Deng, R.; Su, Q.; Wei, Y.; Tang, Y.; Qin, X.; Liu, X. Anomalous upconversion amplification induced by surface reconstruction in lanthanide sublattices. *Nat. Photonics* **2021**, *15* (10), 732-737.
(48) Garfield, D. J.; Borys, N. J.; Hamed, S. M.; Torquato, N. A.; Tajon, C. A.; Tian, B.; Shevitski, B.; Barnard, E. S.; Suh, Y. D.; Aloni, S.; et al. Enrichment of molecular antenna triplets amplifies upconverting nanoparticle emission. *Nat. Photonics* **2018**, *12* (7), 402-407.
(49) LaBoda, C. D.; Dwyer, C. L. Upconverting Nanoparticle Relays for Resonance Energy Transfer Networks. *Adv. Funct. Mater.* **2016**, *26* (17), 2866-2874.
(50) Tao, H.; Wu, T.; Aldeghi, M.; Wu, T. C.; Aspuru-Guzik, A.; Kumacheva, E. Nanoparticle synthesis assisted by machine learning. *Nat. Rev. Mater.* **2021**, *6* (8), 701-716.
(51) Chan, E. M.; Xu, C.; Mao, A. W.; Han, G.; Owen, J. S.; Cohen, B. E.; Milliron, D. J. Reproducible, High-Throughput Synthesis of Colloidal Nanocrystals for Optimization in Multidimensional Parameter Space. *Nano Lett.* **2010**, *10* (5), 1874-1885.
(52) Chan, E. M.; Gargas, D. J.; Schuck, P. J.; Milliron, D. J. Concentrating and Recycling Energy in Lanthanide Codopants for Efficient and Spectrally Pure Emission: The Case of NaYF4:Er3+/Tm3+ Upconverting Nanocrystals. *J. Phys. Chem. B* **2012**, *116* (35), 10561-10570.
(53) Jain, A.; Ong, S. P.; Hautier, G.; Chen, W.; Richards, W. D.; Dacek, S.; Cholia, S.; Gunter, D.; Skinner, D.; Ceder, G.; et al. Commentary: The Materials Project: A materials genome approach to accelerating materials innovation. *APL Materials* **2013**, *1* (1), 011002.
(54) Raccuglia, P.; Elbert, K. C.; Adler, P. D. F.; Falk, C.; Wenny, M. B.; Mollo, A.; Zeller, M.; Friedler, S. A.; Schrier, J.; Norquist, A. J. Machine-learning-assisted materials discovery using failed experiments. *Nature* **2016**, *533*, 73.
(55) Li, Z.; Nega, P. W.; Nellikkal, M. A. N.; Dun, C.; Zeller, M.; Urban, J. J.; Saidi, W. A.; Schrier, J.; Norquist, A. J.; Chan, E. M. Dimensional Control over Metal Halide Perovskite Crystallization Guided by Active Learning. *Chem. Mater.* **2022**, *34* (2), 756-767.
(56) Tom, G.; Schmid, S. P.; Baird, S. G.; Cao, Y.; Darvish, K.; Hao, H.; Lo, S.; Pablo-García, S.; Rajaonson, E. M.; Skreta, M.; et al. Self-Driving Laboratories for Chemistry and Materials Science. *Chem. Rev.* **2024**, *124* (16), 9633-9732.
(57) Epps, R. W.; Volk, A. A.; Ibrahim, M. Y. S.; Abolhasani, M. Universal self-driving laboratory for accelerated discovery of materials and molecules. *Chem* **2021**, *7* (10), 2541-2545.
(58) Bateni, F.; Sadeghi, S.; Orouji, N.; Bennett, J. A.; Punati, V. S.; Stark, C.; Wang, J.; Rosko, M. C.; Chen, O.; Castellano, F. N.; et al. Smart Dope: A Self-Driving Fluidic Lab for Accelerated Development of Doped Perovskite Quantum Dots. *Advanced Energy Materials* **2024**, *14* (1), 2302303.
(59) Chan, E. M. Automated Nanocrystal Synthesis: Lessons from 25 Years of Robots, Microfluidics, and Machine Learning. *Nano Lett.* **2026**, *26* (1), 8-17.
(60) Orimoto, Y.; Watanabe, K.; Yamashita, K.; Uehara, M.; Nakamura, H.; Furuya, T.; Maeda, H. Application of Artificial Neural Networks to Rapid Data Analysis in Combinatorial Nanoparticle Syntheses. *J. Phys. Chem. C* **2012**, *116* (33), 17885-17896.
(61) Krishnadasan, S.; Brown, R. J. C.; deMello, A. J.; deMello, J. C. Intelligent routes to the controlled synthesis of nanoparticles. *Lab Chip* **2007**, *7* (11), 1434-1441, 10.1039/B711412E.
(62) Maceiczyk, R. M.; deMello, A. J. Fast and Reliable Metamodeling of Complex Reaction Spaces Using Universal Kriging. *J. Phys. Chem. C* **2014**, *118* (34), 20026-20033.

(63) Bezinge, L.; Maceiczyk, R. M.; Lignos, I.; Kovalenko, M. V.; deMello, A. J. Pick a Color MARIA: Adaptive Sampling Enables the Rapid Identification of Complex Perovskite Nanocrystal Compositions with Defined Emission Characteristics. *ACS Applied Materials & Interfaces* **2018**, *10* (22), 18869-18878.
(64) Li, J.; Li, J.; Liu, R.; Tu, Y.; Li, Y.; Cheng, J.; He, T.; Zhu, X. Autonomous discovery of optically active chiral inorganic perovskite nanocrystals through an intelligent cloud lab. *Nat. Commun.* **2020**, *11* (1), 2046.
(65) Salley, D.; Keenan, G.; Grizou, J.; Sharma, A.; Martín, S.; Cronin, L. A nanomaterials discovery robot for the Darwinian evolution of shape programmable gold nanoparticles. *Nat. Commun.* **2020**, *11* (1), 2771.
(66) Gleason, S. P.; Dahl, J. C.; Elzouka, M.; Wang, X.; Byrne, D. O.; Cho, H.; Gababa, M.; Prasher, R. S.; Lubner, S.; Chan, E. M.; et al. Automated Gold Nanorod Spectral Morphology Analysis Pipeline. *ACS Nano* **2024**, *18* (51), 34646-34655.
(67) Volk, A. A.; Epps, R. W.; Yonemoto, D. T.; Masters, B. S.; Castellano, F. N.; Reyes, K. G.; Abolhasani, M. AlphaFlow: autonomous discovery and optimization of multi-step chemistry using a self-driven fluidic lab guided by reinforcement learning. *Nat. Commun.* **2023**, *14* (1), 1403.
(68) Levy, E. S.; Tajon, C. A.; Bischof, T. S.; Iafrati, J.; Fernandez-Bravo, A.; Garfield, D. J.; Chamanzar, M.; Maharbiz, M. M.; Sohal, V. S.; Schuck, P. J.; et al. Energy-Looping Nanoparticles: Harnessing Excited-State Absorption for Deep-Tissue Imaging. *ACS Nano* **2016**, *10* (9), 8423-8433.
(69) Jia, X.; Lynch, A.; Huang, Y.; Danielson, M.; Lang'at, I.; Milder, A.; Ruby, A. E.; Wang, H.; Friedler, S. A.; Norquist, A. J.; et al. Anthropogenic biases in chemical reaction data hinder exploratory inorganic synthesis. *Nature* **2019**, *573* (7773), 251-255.
(70) Mehra, S.; Chan, E. M.; Salleo, A. Modular synthetic design enables precise control of shape and doping in colloidal zinc oxide nanorods. *Journal of Materials Chemistry C* **2015**, *3* (27), 7172-7179, 10.1039/C5TC01216C.
(71) Mehra, S.; Bergerud, A.; Milliron, D. J.; Chan, E. M.; Salleo, A. Core/Shell Approach to Dopant Incorporation and Shape Control in Colloidal Zinc Oxide Nanorods. *Chem. Mater.* **2016**, *28* (10), 3454-3461.
(72) Li, S.; Meng, Y.; Guo, Y.; Liu, T.; Stavrakis, S.; Howes, P. D.; deMello, A. J. Precision tuning of rare-earth-doped upconversion nanoparticles via droplet-based microfluidic screening. *Journal of Materials Chemistry C* **2021**, *9* (3), 925-933, 10.1039/D0TC04309E.
(73) Wood, C. H.; Sanchez-Delgado, C. L.; Sternlicht, H.; Soliman, S. S.; Alem, N.; Schaak, R. E. Automated Benchtop Synthesis of a Quadrillion-Plus Member Core@Multishell Nanoparticle Library Using a Massively Generalizable Nanochemical Reaction. *ACS Nano* **2025**.
(74) Zichi, L.; Barter, D.; Sivonxay, E.; Spotte-Smith, E. W. C.; Mohanakrishnan, R. S.; Chan, E. M.; Persson, K. A.; Blau, S. M. RNMC: kinetic Monte Carlo implementations for complex reaction networks. *Journal of Open Source Software* **2024**, *9* (104), 7244.
(75) Szalkowski, M.; Dudek, M.; Korczak, Z.; Lee, C.; Marciniak, Ł.; Chan, E. M.; Schuck, P. J.; Bednarkiewicz, A. Predicting the impact of temperature dependent multi-phonon relaxation processes on the photon avalanche behavior in Tm3+: NaYF4 nanoparticles. *Optical Materials: X* **2021**, *12*, 100102.
(76) Ruan, L.; Zhang, Y. NIR-excitable heterostructured upconversion perovskite nanodots with improved stability. *Nat. Commun.* **2021**, *12* (1), 219.
(77) Xie, T.; Grossman, J. C. Crystal Graph Convolutional Neural Networks for an Accurate and Interpretable Prediction of Material Properties. *Phys. Rev. Lett.* **2018**, *120* (14), 145301.
(78) Chen, C.; Ye, W.; Zuo, Y.; Zheng, C.; Ong, S. P. Graph Networks as a Universal Machine Learning Framework for Molecules and Crystals. *Chem. Mater.* **2019**, *31* (9), 3564-3572.
(79) Li, Z.; Najeeb, M. A.; Alves, L.; Sherman, A. Z.; Shekar, V.; Cruz Parrilla, P.; Pendleton, I. M.; Wang, W.; Nega, P. W.; Zeller, M.; et al. Robot-Accelerated Perovskite Investigation and Discovery. *Chem. Mater.* **2020**, *32* (13), 5650-5663.
(80) Chan, E. M.; Marcus, M. A.; Fakra, S.; ElNaggar, M.; Mathies, R. A.; Alivisatos, A. P. Millisecond Kinetics of Nanocrystal Cation Exchange Using Microfluidic X-ray Absorption Spectroscopy. *J. Phys. Chem. A* **2007**, *111* (49), 12210-12215.
(81) Lookman, T.; Balachandran, P. V.; Xue, D.; Yuan, R. Active learning in materials science with emphasis on adaptive sampling using uncertainties for targeted design. *npj Computational Materials* **2019**, *5* (1), 21.
(82) Kim, M. A.; Ai, Q.; Norquist, A. J.; Schrier, J.; Chan, E. M. Active Learning of Ligands That Enhance Perovskite Nanocrystal Luminescence. *ACS Nano* **2024**, *18* (22), 14514-14522.
(83) Li, X.; Che, Y.; Chen, L.; Liu, T.; Wang, K.; Liu, L.; Yang, H.; Pyzer-Knapp, E. O.; Cooper, A. I. Sequential closed-loop Bayesian optimization as a guide for organic molecular metallophotocatalyst formulation discovery. *Nature Chemistry* **2024**, *16* (8), 1286-1294.
(84) Shields, B. J.; Stevens, J.; Li, J.; Parasram, M.; Damani, F.; Alvarado, J. I. M.; Janey, J. M.; Adams, R. P.; Doyle, A. G. Bayesian reaction optimization as a tool for chemical synthesis. *Nature* **2021**, *590* (7844), 89-96.
(85) Littman, M. L. Reinforcement learning improves behaviour from evaluative feedback. *Nature* **2015**, *521* (7553), 445-451.
(86) Whitelam, S.; Tamblyn, I. Learning to grow: Control of material self-assembly using evolutionary reinforcement learning. *Physical Review E* **2020**, *101* (5), 052604.
(87) Wang, W.; Chen, K.; Ma, X.; Guo, J. Artificial intelligence reinforced upconversion nanoparticle-based lateral flow assay via transfer learning. *Fundam. Res.* **2023**, *3* (4), 544-556.
(88) Pendleton, I. M.; Cattabriga, G.; Li, Z.; Najeeb, M. A.; Friedler, S. A.; Norquist, A. J.; Chan, E. M.; Schrier, J. Experiment Specification, Capture and Laboratory Automation Technology (ESCALATE): a software pipeline for automated chemical experimentation and data management. *MRS Communications* **2019**, *9* (3), 846-859.
(89) Shekar, V.; Nicholas, G.; Najeeb, M. A.; Zeile, M.; Yu, V.; Wang, X.; Slack, D.; Li, Z.; Nega, P. W.; Chan, E. M.; et al. Active meta-learning for predicting and selecting perovskite crystallization experiments. *J. Chem. Phys.* **2022**, *156* (6), 064108.
(90) Chávez, D.; Oliva-Uc, J. R.; Rodríguez-García, C. E.; Castelán, M. A review of artificial intelligence approaches for the development of upconversion and downconversion phosphors. *J. Alloys Compd.* **2026**, *1057*, 186792.
(91) Wen, H.; Luna-Romera, J. M.; Riquelme, J. C.; Dwyer, C.; Chang, S. L. Y. Statistically representative metrology of nanoparticles via unsupervised machine learning of TEM images. *Nanomaterials (Basel)* **2021**, *11* (10), 2706.
(92) Liao, J.; Zhou, J.; Song, Y.; Liu, B.; Lu, J.; Jin, D. Optical Fingerprint Classification of Single Upconversion Nanoparticles by Deep Learning. *J. Phys. Chem. Lett.* **2021**, *12* (41), 10242-10248.
(93) Liu, B.; Liao, J.; Song, Y.; Chen, C.; Ding, L.; Lu, J.; Zhou, J.; Wang, F. Multiplexed structured illumination super-resolution imaging with lifetime-engineered upconversion nanoparticles. *Nanoscale Adv.* **2021**, *4* (1), 30-38.
(94) Đorđević, N.; Beckwith, J. S.; Yarema, M.; Yarema, O.; Rosspeintner, A.; Yazdani, N.; Leuthold, J.; Vauthey, E.; Wood, V. Machine learning for analysis of time-resolved luminescence data. *ACS Photonics* **2018**, *5* (12), 4888-4895.

(95) Liu, Y.; Wu, T.; Zhou, X.; Wang, F. Nonlinear spectral fusion super-resolution fluorescence microscopy based on progressively saturated upconversion nanoparticles. *arXiv [physics.optics]* **2025**.
(96) Wu, S.; Zhou, X.; Kong, W.; Zhao, Y.; Shang, Y.; Zhang, Z.; Liu, Y. Deep learning enhanced dual-mode fluorescence cooperative imaging using upconversion nanoparticles. *Opt. Express* **2025**, *33* (18), 38603-38617.
(97) Mejia-Mendez, J. L.; Reza-Zaldívar, E. E.; Sanchez-Martinez, A.; Ceballos-Sanchez, O.; Navarro-López, D. E.; Marcelo Lozano, L.; Armendariz-Borunda, J.; Tiwari, N.; Jacobo-Velázquez, D. A.; Sanchez-Ante, G.; et al. Exploring the cytotoxic and antioxidant properties of lanthanide-doped ZnO nanoparticles: a study with machine learning interpretation. *J. Nanobiotechnology* **2024**, *22* (1), 687.
(98) Kang, X.; Zhang, Q.; Yang, F.; Li, X.; Jia, W.; Pan, L.; Yang, L.; Jiang, C. Machine learning-coupled upconversion nanoprobe-based immunochromatographic device for blood drug dynamics monitoring. *Adv. Funct. Mater.* **2025**, (e18138).
(99) Ximendes, E.; Marin, R.; Carlos, L. D.; Jaque, D. Less is more: dimensionality reduction as a general strategy for more precise luminescence thermometry. *Light: Science & Applications* **2022**, *11* (1), 237.
(100) Santos, E. P.; Pugina, R. S.; Hilário, E. G.; Carvalho, A. J. A.; Jacinto, C.; Rego-Filho, F. A. M. G.; Canabarro, A.; Gomes, A. S. L.; Caiut, J. M. A.; Moura, A. L. Towards accurate real-time luminescence thermometry: An automated machine learning approach. *Sensors and Actuators A: Physical* **2023**, *362*, 114666.
(101) Zhai, D.; Jing, Y.; Li, X.; Zhang, F.; Wan, T.; Lu, G.; Qin, R.; Jiang, J.; Wang, H. A deep learning based upconversion fluorescence detection system for the detection of gallic acid. *Microchem. J.* **2025**, *217* (114877), 114877.
(102) Yi, Z.; Gao, H.; Ji, X.; Yeo, X.-Y.; Chong, S. Y.; Mao, Y.; Luo, B.; Shen, C.; Han, S.; Wang, J.-W.; et al. Mapping Drug-Induced Neuropathy through In-Situ Motor Protein Tracking and Machine Learning. *J. Am. Chem. Soc.* **2021**, *143* (36), 14907-14915.
(103) Shang, J.; Fang, G.; Yin, X.; Xia, H.; Xue, R.; Wu, J.; Li, Z.; Jing, Y.; Wang, Z.; Zhang, X.; et al. Dynamic multicolor upconversion through excitation pulse duration modulation toward machine learning assisted optical encryption. *Laser Photon. Rev.* **2025**, *19* (17), 2500465.
(104) Leng, Y.-B.; Lv, Z.; Huang, S.; Xie, P.; Li, H.-X.; Zhu, S.; Sun, T.; Zhou, Y.; Zhai, Y.; Li, Q.; et al. A Near-Infrared Retinomorphic Device with High Dimensionality Reservoir Expression. *Adv. Mater.* **2024**, *36* (48), 2411225.
(105) Han, J.; Mao, H.; Lin, Y.; Peng, K.; Meng, L.; Ding, Y.; Shan, X.; Tao, Y.; Shi, J.; Wang, Z.; et al. Near-Infrared Optoelectronic Memristor with All-Optical Modulation for Microscopic Biological Motion Recognition. *Adv. Mater.* **2025**, *37* (45), e10185.
(106) Wu, S.; Zhou, X.; Kong, W.; Zhao, Y.; Shang, Y.; Zhang, Z.; Liu, Y. Deep learning enhanced dual-mode fluorescence cooperative imaging using upconversion nanoparticles. *Opt. Express* **2025**, *33* (18), 38603-38617.
(107) Wang, Y.; Liu, M.; Yang, C.; Jia, Q.; Dai, J.; Li, Z.; Tian, D.; Yan, Z.; Zhang, Y.; Wu, C.; et al. Emerging Upconversion Nanoparticle Hybrid Heterostructures for Advanced Optoelectronic Devices and Intelligent Applications. *Adv. Funct. Mater.* **2026**, *n/a* (n/a), e75431.
(108) Bao, Q.; He, J.; Li, Z.; Bu, Y.; Wang, X. Machine learning prediction and efficient screening method for thermally induced fluorescence enhancement of er^{3}+ doped materials. *Opt. Express* **2025**, *33* (23), 47563-47577.
(109) Shahriari, B.; Swersky, K.; Wang, Z.; Adams, R. P.; de Freitas, N. Taking the Human Out of the Loop: A Review of Bayesian Optimization. *Proceedings of the IEEE* **2016**, *104* (1), 148-175.
(110) Sheng, Z.; Zhu, H.; Shao, B.; He, Y.; Liu, Z.; Wang, S.; Sheng, M. Accelerated discovery of energy materials via graph neural network. *Inorganics (Basel)* **2025**, *13* (12), 395.
(111) Burger, B.; Maffettone, P. M.; Gusev, V. V.; Aitchison, C. M.; Bai, Y.; Wang, X.; Li, X.; Alston, B. M.; Li, B.; Clowes, R.; et al. A mobile robotic chemist. *Nature* **2020**, *583* (7815), 237-241.
(112) Langner, S.; Häse, F.; Perea, J. D.; Stubhan, T.; Hauch, J.; Roch, L. M.; Heumueller, T.; Aspuru-Guzik, A.; Brabec, C. J. Beyond Ternary OPV: High-Throughput Experimentation and Self-Driving Laboratories Optimize Multicomponent Systems. *Adv. Mater.* **2020**, *32* (14), 1907801.
(113) Park, H. S.; Mazaheri, M.; Choi, C.; Hao, H.; Avagliano, D.; Isbrandt, E.; S. B. Karunathilaka, B.; Adachi, C.; Aspuru-Guzik, A. Discovery of tunable and soluble organic emitters for solid-state lasers with a self-driving laboratory. *Nat. Commun.* **2026**.
(114) Fare, C.; Fenner, P.; Benatan, M.; Varsi, A.; Pyzer-Knapp, E. O. A multi-fidelity machine learning approach to high throughput materials screening. *npj Computational Materials* **2022**, *8* (1), 257.
(115) Zeni, C.; Pinsler, R.; Zügner, D.; Fowler, A.; Horton, M.; Fu, X.; Wang, Z.; Shysheya, A.; Crabbé, J.; Ueda, S.; et al. A generative model for inorganic materials design. *Nature* **2025**, *639* (8055), 624-632.
(116) Duan, C.; Liu, G.-H.; Du, Y.; Chen, T.; Zhao, Q.; Jia, H.; Gomes, C. P.; Theodorou, E. A.; Kulik, H. J. Optimal transport for generating transition states in chemical reactions. *Nat. Mach. Intell.* **2025**, *7* (4), 615-626.
(117) Zhang, B.; Summers, T. J.; Augustine, L. J.; Taylor, M. G.; Geist, A.; Li, R.; Batista, E. R.; Perez, D.; Yang, P.; Schrier, J. Augmenting large language models for automated discovery of f-element extractants. *ChemRxiv* **2025**.
(118) Sanchez, S. L.; Kim, Y.; S. Fuhr, A.; Kanyowa, T.; C. Houston, A.; Mokhtarinori, N.; Dubey, A.; Marshall, J.; Puretzky, A.; Duscher, G.; et al. LLM-Guided Ligand Design for Controlling Nanoscopic Morphology of CsPbBr3 Perovskite Nanocrystals. *ChemRxiv* **2025**.
(119) Gottweis, J.; Weng, W.-H.; Daryin, A.; Tu, T.; Palepu, A.; Sirkovic, P.; Myaskovsky, A.; Weissenberger, F.; Rong, K.; Tanno, R.; et al. Towards an AI co-scientist. *arXiv [cs.AI]* **2025**.
(120) Jumper, J.; Evans, R.; Pritzel, A.; Green, T.; Figurnov, M.; Ronneberger, O.; Tunyasuvunakool, K.; Bates, R.; Žídek, A.; Potapenko, A.; et al. Highly accurate protein structure prediction with AlphaFold. *Nature* **2021**, *596* (7873), 583-589.
(121) Wilkinson, M. D.; Dumontier, M.; Aalbersberg, I. J.; Appleton, G.; Axton, M.; Baak, A.; Blomberg, N.; Boiten, J.-W.; da Silva Santos, L. B.; Bourne, P. E.; et al. The FAIR Guiding Principles for scientific data management and stewardship. *Scientific Data* **2016**, *3* (1), 160018.